Geothermics 119 (2024) 102954

Contents lists available at ScienceDirect

Geothermics

journal homepage: www.elsevier.com/locate/geothermics

Shallow geothermal potential and numerical modelling of the geo-exchange for a sustainable post-earthquake building reconstruction (Potenza River valley, Marche Region, Central Italy)

Mario Di Pierdomenico [a], Marco Taussi [a,*], Antonio Galgaro [b], Giorgia Dalla Santa [b,c], Massimiliano Maggini [a], Alberto Renzulli [a,d]

[a] Dipartimento di Scienze Pure e Applicate, Università Degli Studi di Urbino "Carlo Bo", Via Ca' Le Suore 2/4, 61029 Urbino, Italy
[b] Dipartimento di Geoscienze, Università di Padova, Via Giovanni Gradenigo,6, 35131, Padova, Italy
[c] Dipartimento di Ingegneria Civile Edile e Ambientale, Università di Padova, Via Ognissanti 39, 35131, Padova, Italy
[d] Geo.In.Tech. srl Spin Off, Università degli Studi di Urbino Carlo Bo, Via Ca' Le Suore 2/4, 61029 Urbino, Italy

ARTICLE INFO

Keywords:
Shallow geothermal energy
Borehole heat exchangers
Heat pumps
Renewable energy
Thermal conductivity
Numerical modelling

ABSTRACT

The southern part of the Marche Region (Italy) was hit in 2016 by dramatic seismic events that caused damages and fatalities. After these events, the national and local administrations started a development plan to improve the energy efficiency of the restored or reconstructed buildings. Shallow geothermal energy, consisting of closed-loop Borehole Heat Exchangers (BHEs) coupled with heat pumps, could represent a first-order renewable choice for indoor air conditioning (heating and cooling) systems. The feasibility and potential of the BHEs also match this technology's null visual outdoor impact which is paramount in preserving the landscape of the earthquake-affected areas. However, the exploitation, sustainability, and correct design of these systems require detailed knowledge of the ground's geological, hydrogeological, and thermophysical properties. In this framework, the present study was carried out to map and test, through the G.POT algorithm, the shallow geothermal potential and sustainability of the Potenza River valley through the publicly available data from the Italian Seismic Microzonation studies — an extensive database of geognostic drillings and other geological and geophysical surveys. This step allowed us to assign the main thermal parameters (thermal conductivity, volumetric heat capacity, specific heat extracted) to each geological layer and averaged them over the first 100 m (i.e., a typical depth for BHEs). All the data were then interpolated to produce geothermal thematic maps to visualize and compare the potential and adequacy of the territory for the installation of closed-loop BHEs. Finally, finite elements numerical models (FEFLOW® software) were developed in a balanced mode through the annual heating and cooling cycles to verify the sustainability of this renewable concerning the thermal impact induced to the ground by the BHEs during a long-term (20 years) operation.

1. Introduction

In 2016, Central Italy was hit by a seismic sequence (M_{max} 6.5) that caused human victims, damages, and building collapses, hopelessly changing the urban landscape of many towns (INGV, 2016). After these events, the Marche Region, the most affected area together with Abruzzo, Umbria, and Lazio Regions, started an economic program that involved measures for the restoration and reconstruction of damaged or destroyed buildings (USR, 2016). The reconstruction of the affected areas is addressed to renewable-sustained, self-sufficient, and environmentally friendly new buildings. In this framework, the exploitation of shallow ground heat exchange through the installation of closed-loop Borehole Heat Exchangers (BHEs) coupled with heat pumps could be a tool of paramount importance for indoor air conditioning systems (heating and cooling) for these new or renovated buildings, as occurred in other similar situations (e.g., in New Zealand after the 2011 Christchurch earthquake; Daysh et al., 2021). Closed-loop BHE systems mainly consist of a series of probes inserted into the ground, down to 80–120 m of depth or more, where a heat carrier fluid flows into the probes, thus allowing the heat exchange between the ground and the

* Corresponding author.
E-mail address: marco.taussi@uniurb.it (M. Taussi).

https://doi.org/10.1016/j.geothermics.2024.102954
Received 16 October 2023; Received in revised form 8 January 2024; Accepted 6 February 2024
Available online 12 February 2024

served building at the surface (e.g., Muñoz et al., 2015; Piscaglia et al., 2016; Soltani et al., 2019; Galgaro et al., 2021). The same system can be used both in winter and summer. A ground source heat pump manages the temperature and the discharge of the heat carrier fluid to meet the building's thermal needs. These indoor heating and cooling systems through closed-loop BHEs have very low or no environmental impact and are increasingly developing in Italy and worldwide (Manzella et al., 2018; Lund and Toth, 2021). Closed-loop BHE systems represent an almost carbon-free renewable able to produce clean thermal energy with a high coefficient of performance (COP) and an almost null visual impact, therefore strongly contributing to preserving the landscape. Although the BHEs can be developed almost everywhere, their efficiency and thermal impact on the ground are directly related to the knowledge of the thermal properties of the different lithologies and the hydrogeological setting, which strongly influence the total amount of heat (and cold) that can be extracted or reinjected (e.g., Schiermeier et al., 2008; Muñoz et al., 2015). Thus, an in-depth knowledge of the geological features and a correct design of the geometric distribution of the BHEs and the operational conditions of the heat pump throughout the annual heating and cooling cycles are required to avoid a loss of efficiency. Nonetheless, the continued heat exchange with the ground could cause, with time, a thermal alteration of the ground itself and the aquifers (Piscaglia et al., 2016; Bayer et al., 2019; Gizzi et al., 2020; Perego et al., 2022; Muñoz et al., 2023). In this case, an essential tool to know and foresee the thermal plume development in the ground involved in the heat exchange during a distinct time interval is the numerical modelling (Diersch et al., 2010; Halaj et al., 2020;), which can predict the thermal modifications of the ground system. In this framework, the main goal of this study is to define and map the BHE-installation potential along the Potenza River valley, an area that suffered severe damages from the seismic sequence that occurred in 2016 and characterized by a heterogeneous geological setting representative of the variable conditions occurring in the southern part of the Marche Region. The study area has a good availability of publicly accessible data related to the Italian Seismic Microzonation studies (TCSM, 2018), which were used to characterize the ground. These studies, carried out to assess the local seismic hazard through the identification of areas of the territory characterised by homogeneous seismic behaviour, contain an extensive geological database made of geognostic drillings, penetrometric tests, and geophysical surveys, among others, that indeed can be exploited for different scopes (Moscatelli et al., 2020; Taussi et al., 2021). The extensive database was used to (1) define the subsoil stratigraphy, (2) create thematic maps of the local shallow geothermal potential, and (3) support the numerical models developed to check the sustainability of BHE systems in the long term.

In the first phase, the underground's main geological, hydraulic, and thermophysical properties were defined and assigned to the different stratigraphic layers. This first characterization allowed the production of thematic maps of the thermal properties by using ArcGIS 10.8.2 software and estimating the geothermal potential of the area, intended as the indicator of the efficiency and long-term sustainability of a BHE implementation (Casasso and Sethi, 2016). In the second phase, detailed simulations of vertical closed-loop BHEs were carried out in the seven municipality's territories of the Potenza River valley. In each of them, the installation of the same closed-loop BHE system was assumed (i.e., three probes of 100 m depth, with Double-U configuration) to evaluate and compare how the different geological settings would have affect the efficiency of the BHEs (e.g., Blasi and Menichetti, 2012; Galgaro et al., 2021; Kerme and Fung, 2021; Gigot et al., 2023). The ground temperature variations and the thermal plumes produced by the operation of the BHE, coupled with fixed 12-kW heat pumps through a 20 years simulation time interval, were calculated using a finite element software (FEFLOW®, MIKE Powered by DHI Software) permitting to faithfully reproduce the undisturbed conditions of the site and any effects in the shallow ground, over time, of the closed-loop heating and cooling system.

The outcome of this study aims to support the use of BHE systems and investments in this renewable also to achieve the objectives of the United Nations Sustainable Development Goal 7 (Affordable and Clean Energy; https://www.un.org/sustainabledevelopment/energy/). Moreover, it can provide an opportunity for designers, decision-makers, and administrative authorities to evaluate and have an awareness of the shallow geothermal potential (i.e., geo-exchange; Viesi et al., 2018) during the post-earthquake restoration and reconstruction activities of damaged or destroyed buildings in the Potenza River valley and more generally in the whole area of southern Marche Region.

2. Study area and geological background

The Potenza River valley develops on the Adriatic side of the central Apennines (Fig. 1a) and crosses from west to east, predominantly mountainous and hilly areas, respectively. The valley (about 200 km^2) lies between the town of Fiuminata to the west and the city of Macerata to the east (Fig. 1b). In between, five other municipalities occur: Pioraco, Castelraimondo, Gagliole, San Severino, and Pollenza. About 66,000 people live in this area (ISTAT, 2021). The eastern side of the Central Apennines chain is characterized by an estimated surface conductive heat flow ranging between 30 and 50 mW m^{-2} (Pauselli et al., 2019; Verdoya et al., 2021; Santini et al., 2021). Lithologies of this area are linked to the geological history of the so-called Umbria-Marche succession (e.g., Conti et al., 2020 and references therein), characterized by sedimentation of pelagic carbonates (limestones and marly limestones) since the Jurassic and continuing until the Paleogene, as the result of distensive processes. These latter were firstly induced by the opening of the Ligurian Ocean (Neotethys domain) and, later, by both thermal subsidence and tectonic thinning of the paleo-margin (Cello et al., 1996; Tavarnelli, 1997). From the Miocene, this succession of the African-Adriatic continental margin was involved in the structuring of the Apennine thrust system, which, in the study area, began at the Miocene-Pliocene transition (Ricci, 1986; Calamita et al., 1994; Vezzani et al., 2010), with continuous reorganization of the foreland areas and dominated by turbiditic successions (Marcheggiani et al., 1999; Bigi et al., 1999) (Fig. 1).

All the Potenza River valley geological formations are comprised between the Maiolica Fm (Early Tithonian p.p.-Early Aptian) and the Argille Azzurre Fm (Pliocene-Pleistocene p.p.). In detail, they are represented by (Conti et al. (2020): (1) well-bedded limestones, marly limestones, and marls (Cretaceous-Early Miocene units: Maiolica, Marne a Fucoidi, Scaglia Bianca, Scaglia Rossa, Scaglia Variegata, Scaglia Cinerea, Bisciaro, and Schlier Fms), and (2) sandstones and siltstones with interbedded marlstones (Miocene units: Marnoso Arenacea Fm). Tectonically, the area is characterized by a set of anticlines and synclines that overlapped progressively to the east above the turbiditic sediments of the Laga basin (outside the study area) along an NNW-SSE overthrust front. The foreland sectors of the investigated area are characterized by evaporites, clays, and silty clays interbedded with sandstones of the Late Miocene-Pliocene units of the San Donato, Colombacci, and Argille Azzurre Fms (Fig. 1b). The Potenza River valley develops orthogonal to the coastline of the Adriatic Sea and transversely crosscuts the main NE-verging geological structures. The Quaternary deposits comprised within the valley mainly consist of coarse grain size material (gravel to gravelly sand) and gravelly clay with intercalated sand, silty-clay, and sandy silt, which host a phreatic aquifer system (Nanni, 1985).

3. Materials and methods

The methodological approach consisted of the creation of a database containing the fundamental geological, hydrogeological, and stratigraphical information — retrieved from the Italian Seismic Microzonation database (DPC, 2019) — and the thermophysical properties of the ground characterizing the selected municipalities of the Potenza

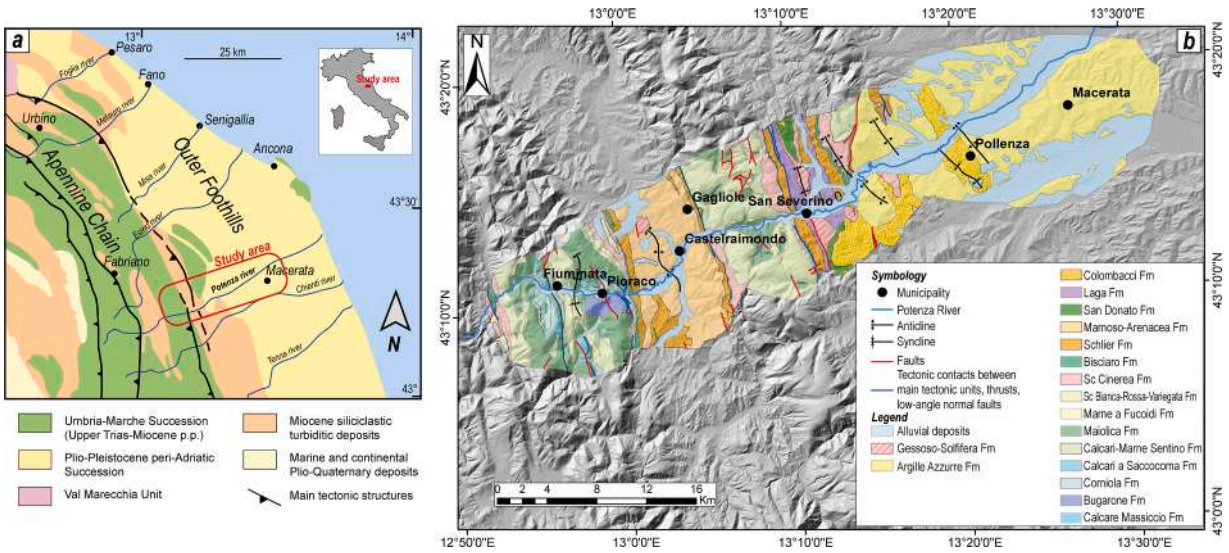

Fig. 1. a) Schematic geological map of the Umbria-Marche Apennines (modified from Chicco et al., 2019a) with the study area represented by the red rectangle; b) simplified geological map of the Potenza River valley (modified after Conti et al., 2020).

River valley (Macerata, Pioraco, Pollenza, Gagliole, Castelraimondo, San Severino, and Fiuminata). The adopted methodology is based on three steps as suggested by Viesi et al. (2018) and already used in several works (e.g., Taussi et al., 2021; Ramos-Escudero et al., 2021; Vespasiano et al., 2023): (1) data collection, (2) production of thematic maps, and (3) evaluation and mapping of geothermal potential (i.e., BHEs potential). The latter was estimated through the G.POT algorithm defined by Casasso and Sethi (2016), which is based on the thermal properties of the ground and the operational and design parameters of the closed-loop geothermal system. The thematic maps were constructed by considering the following properties: (1) climatic conditions (air temperature), (2) subsurface stratigraphy, (3) hydrogeological setting of the area, and (4) thermophysical properties of the lithologies. Thermal conductivity (λ), volumetric heat capacity (SVC), specific heat extraction (SHE) values, and hydrogeological conditions were assigned to each stratigraphic layer based on the available literature data and integrated over the first 100 m of depth to obtain the thematic maps. This depth was chosen because it is the typical reference depth of many closed-loop systems with vertical BHEs (e.g., Hecht-Méndez et al., 2013; Garcia-Gil et al., 2015; Viesi et al., 2018; Ramos-Escudero et al., 2021; Taussi et al., 2021; Barbieri et al., 2022; Vespasiano et al., 2023; Alcaraz and Vives, 2023). All the maps were georeferenced in the WGS84 coordinates system and obtained in ArcGIS by applying a Simple Kriging geostatistical interpolation, which has been used in similar works (e.g., Sáez Blázquez et al., 2022) and representing a precise and robust technique that permitted estimating the values in those areas where no drillings were present (semi-variograms and error maps are reported in the Supplementary Material). The geological map was also considered to better approximate the different interpolated values. After this stage, the data retrieved from the assessment of the area's geological, hydrogeological, and thermal features were used as a starting point for the numerical model simulations. These latter were carried out to compare the geothermal potential of the seven municipalities of the Potenza River valley. Closed-loop BHE systems (one for each municipality) were simulated using FEFLOW software (Diersch, 2014), considering the same operational features and the peculiar settings of each site.

3.1. Surface air temperature

Climatic data, consisting of mean air temperature throughout the study area, were defined using the empirical formula proposed by Gemelli et al. (2011). These authors calculated the surface air temperature (SAT) based on the data acquired from the Meteo-climatological Monitoring Network of the Marche Region and averaged over the period 1950–2000. A numerical relationship between altitude and SAT was established by applying a third-order polynomial regression as follows (Gemelli et al., 2011):

$$SAT = -4 \times 10^{-9} Z^3 + 6 \times 10^{-6} Z^2 - 5.8 \times 10^{-3} Z + 14.703 \quad (1)$$

where Z is the altitude of the weather station. Based on this function, a thematic map was created to associate the altitude of each DEM cell (resolution 10 × 10 m, see Supplementary Material; Tarquini et al., 2023) with the related mean annual temperature (Fig. 2). The temperatures tend to decrease from east to west, i.e., from the lower-altitude areas to the higher ones, starting from an annual mean maximum temperature of 13.6 °C to a minimum of 8.7 °C. These values were then considered for the estimation of the undisturbed soil temperature of the study area, given the fact that in the absence of significant local geothermal anomalies (as in the present work), the annual average temperature of the first 100 m of the underground can be supposed similar, or slighlty higher, to the mean annual air temperature (Viesi et al., 2018). The estimated air temperature values have also been used as the starting temperatures for developing numerical models (see Section 3.6). It is important to note that in the study area, the possible effect of Urban Heat Island (UHI) on the ground temperature (e.g., Bayer et al., 2016; Rivera et al., 2017) was not taken into account because all the seven municipalities are small (<40,000 inhabitants) and thus a negligible UHI effect was considered.

3.2. Hydrogeological data

The amount of heat exchanged and the energy performance of the whole closed-loop BHEs system is strongly influenced by the heat exchange capacity of the ground surrounding the BHEs (e.g., Sarbu and Sebarchievici, 2014; Verdoya and Chiozzi, 2018). In addition, the water table's depth, the presence of aquifers, and groundwater flow characteristics are essential for evaluating this process (Garcia-Gil et al., 2015). Water Protection Plan of the Marche Region (PTA, 2002) gives some information on the hydrogeological setting of the investigated area though no recent hydrogeological studies are present in the literature, to the best of our knowledge. However, the PTA does not include a georeferenced map and is available at a large scale (1:100.000), thus not

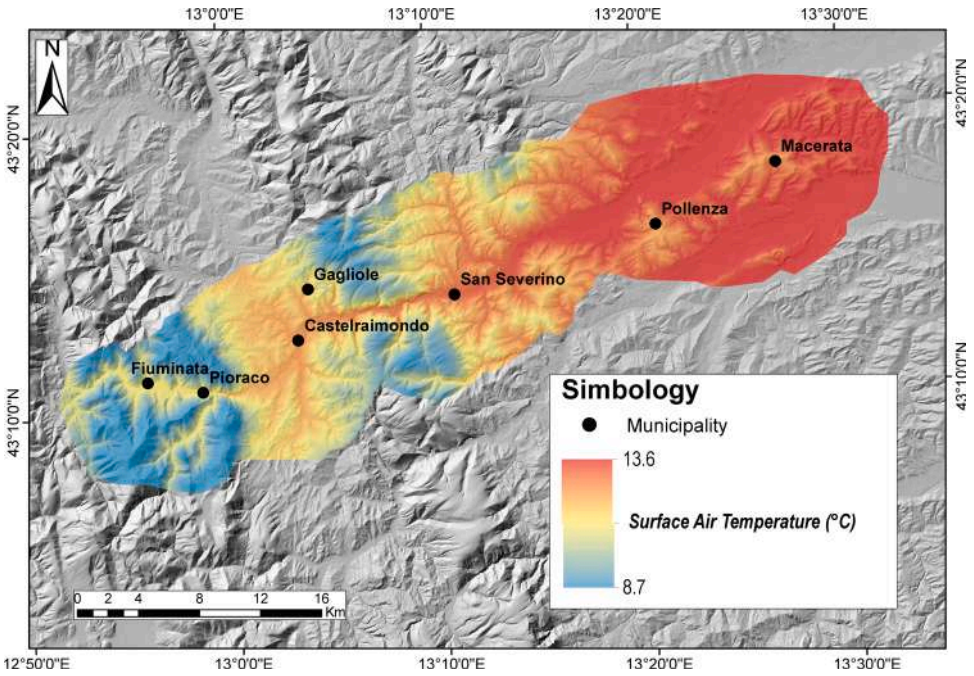

Fig. 2. Surface mean annual Air Temperature of the study area following the equation proposed by Gemelli et al. (2011).

providing a detailed reconstruction of the hydrogeological setting of the area. Consequently, data extracted from the consultation of the drilled cores and penetrometric tests available from the Seismic Microzonation database were used (when reported) to define the saturation conditions of the investigated stratigraphic vertical column.

3.3. Lithostratigraphic data

The geology and stratigraphy of the bedrock in the investigated area were reconstructed based on drilling data, field observations, and the geological map of Conti et al. (2020). In the Italian Seismic Microzonation database, different types of geognostic surveys (e.g., seismic, geotechnical, hydrogeological) are reported. In this study, geognostic drillings were considered because they have less risk of interpretation errors compared to, e.g., Cone Penetration Tests and Dynamic Penetration Super-Heavy Tests, among others. More than 300 drillings were analysed and interpreted, in addition to fieldwork consisting of identifying and localizing rock outcrops in the area. All the selected geognostic drilling reached the bedrock, which is always encountered before 100 m (maximum depth 50 m). Each stratigraphy was thus virtually extended to the required depth, considering homogeneous lithostratigraphic features of the crossed bedrock (e.g., Viesi et al., 2018; Taussi et al., 2021; Vespasiano et al., 2023). The classification of soils used for the Seismic Microzonation studies and defined by the Technical Commission for Seismic Microzonation (TCSM, 2018) follow the modified ``Unified Soil Classification System'' (ASTM, 1985) and is based on the dominant lithology of the alluvial deposits (e.g., gravels, sands, silts, and clays). The geological bedrock is classified based on lithology, stratification, and degree of fracturing. The 16 types of soil proposed by the TCSM (2018) have been grouped and simplified into three categories (sand, gravel, clay/silt) based on the dominant grainsize, following the approach by Taussi et al. (2021), while the bedrock was defined based on the geological map and field observation of the outcrops (Fig. 1).

3.4. Thermophysical properties of the ground

The main thermophysical properties here considered were: i) thermal conductivity (λ), ii) specific heat extraction (SHE), and iii) volumetric heat capacity (SVC). The thermal conductivity values (expressed in W m^{-1} K^{-1}) of the rocks of the Umbria-Marche sedimentary succession were retrieved by various authors (Blasi and Menichetti 2012; Verdoya et al., 2018; Chicco et al., 2019b), while those related to the Quaternary unconsolidated deposits were extracted from the VDI 4640 (2001) and following Dalla Santa et al. (2020). The SVC values (expressed in MJ m^{-3} K^{-1}) were obtained from Andújar-Márquez et al. (2016). Finally, SHE values (expressed in W m^{-1}) were calculated from the relationship defined by Viesi et al. (2018). This correlation between the SHE rates defined by the VDI 4640 (2001) and the thermal conductivity of the different lithologies considered was based on an operational time of 2400 h, as suggested by Gemelli et al. (2011) for the Marche region, and permits defining detail values of the specific case SHE:

$$SHE(2400h) = 3.34\lambda^2 + 4.54\lambda + 21.63 \quad (2)$$

The used values of λ, SVC, and SHE for the different types of lithotypes and unconsolidated sediments (considering saturated or unsaturated conditions) are summarized in Table 1 and do not consider the convection contribution to heat transfer that may be derived from groundwater flow.

3.5. G.POT empirical method

Casasso and Sethi (2016) developed the G.POT (Geothermal POTential) empirical model, a quantitative method to assess the BHE potential using analytical heat transfer simulations. This method allows estimating and mapping, at a regional scale, the shallow geothermal potential (i.e., geo-exchange) to be applied to installing closed-loop BHEs coupled with heat pumps for heating and cooling air conditioning systems. The model assumes that the final potential mainly depends on the site–specific parameters of the shallow ground and its usage patterns. The method provides the annually averaged thermal load (Q_{BHE}) exchangeable between a BHE and the shallow ground and it is eventually solved by calculating the benchmark temperature, leading to the maximum temperature increment of the heat carrier fluid according to the following formula (Casasso and Sethi, 2016):

Table 1
Thermophysical properties of the unconsolidated sediments and lithotypes of the study area.

	Thermal conductivity - λ (W m^{-1} K^{-1})	Thermal conductivity reference	Specific heat extraction (2400 h) - SHE (W m^{-1})[a]	Volumetric heat capacity - SVC (MJ m^{-3} K^{-1})[b]
Unconsolidated sediments				
Gravel dry	0.40	Dalla Santa et al. (2020)	24	1.6
Gravel water-saturated	1.80	VDI 4640 (2001)	41	2.4
Sand dry	0.40	Dalla Santa et al. (2020)	24	1.6
Sand water-saturated	2.40	VDI 4640 (2001)	52	2.9
Clay / silt dry	0.50	VDI 4640 (2001)	25	1.6
Clay / silt water-saturated	1.70	VDI 4640 (2001)	39	3.4
Lithotype				
Argille Azzurre Fm	1.91	Chicco et al. (2019b)	42	2.4
Colombacci Fm	1.96	Blasi (2012)	43	2.4
Laga Fm	2.04	Chicco et al. (2019b)	44	2.5
Marnoso Arenacea Fm	2.10	Blasi and Menichetti (2012)	46	2.6
Schlier Fm	2.18	Verdoya et al. (2018)	47	2.5
Bisciaro Fm	1.32	Chicco et al. (2019b)	33	2.4
Sc. Cinerea Fm	2.10	Chicco et al. (2019b)	46	2.5
Sc. Bianca-Rossa-Variegata Fms	2.09	Chicco et al. (2019b)	46	2.4
Marne a Fucoidi Fm	2.28	Chicco et al. (2019b)	49	2.5
Maiolica Fm	2.27	Chicco et al. (2019b)	49	2.4

[a] based on Eq. (2).
[b] from Andújar-Márquez et al. (2016).

$$Qbhe = \frac{\alpha \cdot (T_0 - T_{lim}) \cdot \lambda \cdot L \cdot t'c}{-0.619 \cdot t'c \cdot \log(u's) + (0.532 \cdot t'c - 0.962) \cdot \log(u'c) - 0.455 \cdot t'c - 1.619 + 4\pi \cdot \cdot Rb} \quad (3)$$

where T_0 and T_{lim} are the soil temperature (derived from Fig. 2) and benchmark temperature of the carrier fluid respectively (°C); λ is the thermal conductivity (in W m^{-1} K^{-1}); L is the BHE length (m); Rb is the thermal resistance of the borehole (in mK W^{-1}); and $t'c$, $u's$, and $u'c$ are dimensionless values depending on the simulation time and the length of the load cycle. Some variables are kept constants (threshold fluid temperature, borehole depth, borehole radius and section, borehole thermal resistance, and the simulated time; Table 2) while the others (thermal conductivity, thermal capacity, and undisturbed ground temperature) are defined for each investigated point. The G.POT method has been widely used to estimate the geo-exchange potential for the heating mode. In our case, the G.POT was applied in dual mode, considering the need for geothermal energy utilisation for both heating and cooling. In this way, operation in cooling mode allows the re-injection of heat into the ground to be used during the winter, reducing the thermal drift of the ground. The threshold temperature of the fluid was determined for both operative modes. The parameters used for applying the G.POT algorithm are summarised in Table 2.

3.6. Numerical models

3.6.1. Construction of the 3D model geometry and mesh

A finite element model of a standard closed-loop system consisting of three BHEs of 100 m was built and run considering the different geological settings, finally comparing the obtained results. To develop the finite element mesh for the FEFLOW software (Diersch, 2014), defining the boundaries of the study area was necessary by manually inserting "superelement" meshes. The domain is rectangular, with the major axis parallel to the groundwater flow hypothesized direction and equal to about 800 m and the minor perpendicular axis of about 400 m (Fig. 3a). In addition to the sides of the computational domain, the installation coordinates of the three BHEs with a triangular geometry equidistant 8 m were also initially defined as elements of the "superelement" meshes. Another file of the same type was created from the latter, but only with the geometry of the BHEs and monitoring wells. A hexagon of points equidistant 0.8 m to aid the meshing process was assigned to each BHE to ensure model convergence, thus obtaining a uniform discretization near the latter (Halaj et al., 2020).

After entering the "superelements", the mesh generation was produced. At this stage, the domain is divided into several finite elements, defining the final simulation's accuracy. The used meshing shape was triangular, with the minimum angle of the elements equal to 29° (Diersch, 2014). The main mesh was divided into a square of 20,000 m^2, in which a second mesh was processed to increase the number of finite elements and, thus, the accuracy of the results. Triangles that violated Delaunay's criterion (Halaj et al., 2020) were refined so that an optimal prism size and a smoother mesh could be obtained, thus defining the three-dimensional model of the domain. The slices were placed in direct correspondence with property changes (physical, thermal, or boundary conditions) of the various deposits and near them to facilitate the convergence of the numerical solver. Given the depth of the probes of 100 m, a 120 m-deep model was defined (Fig. 3b).

On the other hand, according to the division into the slice and layer, the stratigraphic logs of the different municipalities were consulted. The models were divided according to (1) stratigraphic sequence, (2) hydraulic conditions, and (3) BHE bottom (Table 3) of each test site, based on the available geognostic drillings. Permeability and porosity values

Table 2
Closed-loop BHEs (double-U) systems and heat-exchange constant parameters used in the Geothermal POTential (G.POT) algorithm.

Parameter	Symbol	Value	Unit
Threshold fluid temperature (heating mode)	T_{lim}	−2	°C
Threshold fluid temperature (cooling mode)	T_{lim}	35	°C
Borehole depth	L	100	m
Borehole radius	r_b	0.075	m
Simulated lifetime	t_s	50	years
Borehole thermal resistance	R_b	0.1	mK W^{-1}

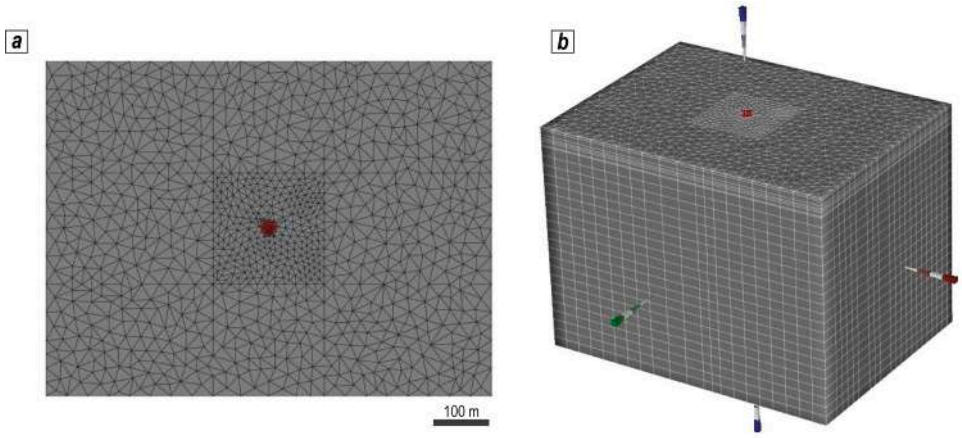

Fig. 3. a) Mesh performed within the calculation domain using FEFLOW software. The domain is divided into a series of finite elements; the triangles produced are responsible for the variables calculation; b) example of a 3D layer configuration; the model was divided according to (1) important changes in hydraulic properties, (2) thermal properties, (3) the base of the BHEs, and (4) calculation conditions.

Table 3
Slice and layer division, simplified stratigraphy, and hydraulic conditions of the seven, 100 m-depth, closed-loop BHEs systems hypothesized for each municipality.

Municipality	Slices	Layers	Depth (m)	Stratigraphy	Permeability (m s^{-1})	Porosity (%)	Hydraulic conditions
Castelraimondo	26	25	0–7.1	Silt	1×10^{-8}	30	0–1.6 dry
			7.1–100	Marnoso-Arenacea Fm	1×10^{-9}	40	1.6–7.1 wet
							7.1–100 dry
Pollenza	29	28	0–0.8	Gravel	1×10^{-3}	35	0–4.7 dry
			0.8–3.0	Sand	1×10^{-7}	40	4.7–8 wet
			3.0–12	Silt	1×10^{-8}	30	8–100 dry
			12–100	Colombacci Fm	1×10^{-10}	15	
Macerata	30	29	0–4.0	Silt	1×10^{-8}	30	0–10 dry
			4.0–15	Sand	1×10^{-7}	40	10–15 wet
			15–100	Argille Azzurre Fm	1×10^{-12}	45	15–100 dry
Pioraco	30	29	0–9.0	Silt	1×10^{-8}	30	0–7.4 dry
			9.0–100	Marnoso Arenacea Fm	1×10^{-9}	40	7.4–8.4 wet
							8.4–100 dry
San Severino	23	22	0–2.5	Silt	1×10^{-8}	30	0–5.3 dry
			2.5–7.5	Gravel	1×10^{-3}	40	5.3–7.5 wet
			7.5–100	Laga Fm	1×10^{-10}	25	7.5–100 dry
Gagliole	24	23	0–5.7	Silt	1×10^{-8}	30	0–2.5 dry
			5.7–100	Schlier Fm	1×10^{-11}	42	2.5–5.7 wet
							5.7–100 dry
Fiuminata	25	24	0–2.3	Silt	1×10^{-8}	30	0–0.9 dry
			2.3–5.0	Clay	1×10^{-11}	45	0.9–2.3 wet
			5.0–100	Marne a Fucoidi Fm	1×10^{-10}	20	2.3–100 dry

were assigned to each layer according to the literature (Morris and Johnson, 1967; Clauser, 2011; Di Sipio et al., 2013; Dalla Santa et al., 2020) (Table 3).

3.6.2. *Building heating and cooling requests*

The power output of each BHE array was defined by simulating the power loads required to meet the needs of a building consisting of three BHEs coupled with a heat pump of 12 kW, which could be considered as an average thermal power demand for a domestic house of 100 m^2 in the study area (Gemelli et al., 2011). Despite the possible slightly different thermal needs of the investigated area, the power demand was maintained constant in all the numerical models. This choice was driven by the fact that i) many buildings need to be restored or reconstructed after the 2016 earthquakes and thus it is not possible to define the new thermal needs *a priori* and ii) to better emphasize the different characteristics of the ground and their influence on the geo-exchange potential. Therefore, we considered a thermal request profile that is typical of a standard residential building in this area, given that the seven municipalities are not so distant from each other (maximum ~45 km before Fiuminata and Macerata; Fig. 1) and located at the same latitude and similar altitudes; thus, they can be associated to the same climatic area.

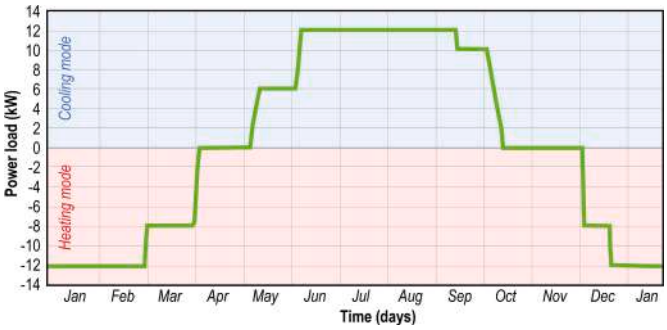

Fig. 4. Time series of the daily variation of the power load exchanged with the ground by the closed-loop BHEs systems. A monthly subdivision is reported for clarity. Positive and negative values refer to cooling and heating modes, respectively.

A file containing the average daily power (in kW) for a year based on seasonality was created. In this way, the equality of the total energy exchanged with the ground is maintained, also achieving higher stability

of the numerical calculation since the objective is the analysis of the induced thermal alteration and the assessment of the BHE sustainability in the long term under quasi-stationary conditions (Halaj et al., 2020; Ramos-Escudero et al., 2021). On the other hand, the description of operations during peak power is lost, which in any case should have a low influence, considering the long-time scale. The time series for both the heating and cooling air conditioning system of a building were calculated considering a 12-kW heat pump modulating the power during the year (Fig. 4). The different power loads during the year were selected according to Lisoet al. (2011) and Bee et al. (2019). The three vertical BHEs were placed at the indicated locations (i.e., with a triangular geometry and 8 m afar from each other) and connected in three BHE arrays, to which an operating fluid flow rate of a total of 0.8 L s^{-1} was assigned for the closed-loop BHEs system. The flow rate was kept constant throughout the simulation, and the same heating and cooling demand was applied to all the simulated closed-loop BHE systems.

3.6.3. Boundary and initial conditions and outcomes of the numerical models

Flow and heat transport features were entered into the models as boundary and initial conditions. In the flow-related boundary condition, a first type (Dirichlet) condition was assigned to each model, while the hydraulic load was assigned to the edges of the reference slices. The second boundary condition was the "hydraulic head" condition in the "process variable" in which an intermediate value was assigned based on the available geognostic drilling data. In all models, the water table is confined to the first 15 m depth, with an average thickness of ~3 m (Table 3). Regarding heat transport, a first type condition was assigned, with the "temperature boundary conditions" tool in heat transport. The only geometric limit of the model is the inlet of the groundwater flow, which helps define the water inlet temperature. Finally, the initial temperature conditions were defined along the entire vertical line of the ground, assigning a temperature like that of the surface air temperature to the first 5 m (Fig. 3). In the subsequent 115 m of the numerical models, the temperature gradually increased by 2–2.5 °C, considering an average geothermal gradient (Della Vedova et al., 2001; Pauselli et al., 2019; Santini et al., 2021). The latter was assigned at the base of the model, according to Pauselli et al. (2019), through the second type condition (Neumann) in "heat transport" (0.06 W m^{-2}). It is worth to note that in some cases, a non-linear temperature gradient with decreasing temperatures in the first 40–50 m of depth likely due to cold groundwater flow was recognized (e.g. Verdoya et al., 2018). However, in the present work we choose to consider a slight increase of the ground temperature with depth because available thermal response test and temperature measurements carried out in similar geological contexts (e.g., Galgaro et al., 2021; Dalla Santa et al., 2022) and in the Marche Region (Menichetti and Renzulli, 2009; Menichetti et al., 2009; Blasi and Menichetti, 2012; Piscaglia et al., 2016; Galgaro et al., 2021) recorded undisturbed temperatures of the first 100–150 m of the ground similar to the local atmospheric one or higher.

Finally, "double U-shaped" pipes were chosen via the fourth type condition, with the BHEs key (Table 4). The quasi-stationary method (Eskilson and Claesson, 1988), which assumes the local thermal equilibrium between all the elements of BHEs during the simulation time, was applied (Halaj et al., 2020).

Table 4
Closed-loop BHEs (double-U) systems settings used in the numerical modelling.

Parameter	Value
Borehole diameter	0.15 m
Intel pipe diameter	0.032 m
Refrigerant volumetric heat capacity	4 MJ m^{-1} s^{-1} K^{-1}
Refrigerant thermal conductivity	0.48 J m^{-1} s^{-1} K^{-1}
Computation method	Eskilson and Claesson (1988)
Net power load	Max 12 kW
Operating fluid flow rate	0.8 l s^{-1}

The numerical modelling gave each municipality's average ground temperature and BHE inlet/outlet temperatures. The first one represents the average temperature (°C) of the subsurface subject to heat exchange over time (20 years), considering the entire investigated column, while the second represents the temperature (°C) of the inlet and outlet operating fluid over the same period.

The graphs obtained from each simulation have been compared, considering the maximum and minimum temperatures reached by the heat transfer fluid, and were used to identify the most favourable locations for a better performance of the system in terms of energy efficiency and reduction of electrical energy used for the heat pump to reach the air conditioning temperatures.

4. Results and discussion

4.1. Thermal conductivity (λ) and volumetric heat capacity (SVC) of the ground

These thermophysical properties were defined in detail for each lithostratigraphic unit identified by the geognostic drillings and averaged over the first 100 m of the ground and reported in Fig. 5a (λ) and b (SVC) maps.

The λ values of the ground averaged over 100 m of depth vary between 1.65 and 2.25 W m^{-1} K^{-1}. The thermal conductivity map (Fig. 5a) shows how the value increases moving inland from the coast (from East to West). The easternmost municipalities (Macerata and Pollenza) are those with relatively low values (<1.80 W m^{-1} K^{-1}) due to the high thicknesses (up to 15 m) of unconsolidated deposits (Table 3) and the relatively low thermal conductivity value of the bedrock, generally represented by the Argille Azzurre (1.91 W m^{-1} K^{-1}) and Colombacci Fms (1.96 W m^{-1} K^{-1}) (Fig. 1b, Table 1). Similarly, in the Pioraco area, the unconsolidated deposits reach about 9 m of thickness, and the thermal conductivity is, on average, about 1.94 W m^{-1} K^{-1}. In the area between San Severino and Castelraimondo (Fig. 5a), the thermal conductivity increases up to 2.14 W m^{-1} K^{-1}, being mainly influenced by the rock type, generally represented by Schlier, Marnoso-Arenacea and Laga Fms (Table 1). In fact, towards the west, the thickness of the alluvial deposits thins out and tends to slightly influence the value of λ in the first 100 m depth. The highest thermal conductivity values are recorded near the municipality of Fiuminata (>2.14 W m^{-1} K^{-1}) (Fig. 5a) due to the presence of the Marne a Fucoidi Fm characterized by higher thermal conductivity (2.28 W m^{-1} K^{-1}) (Table 1).

The volumetric heat capacity (SVC) map (Fig. 5b) shows how a gradual increase from the municipality of Macerata to the East (2.25 MJ m^{-3} K^{-1}) toward the municipality of San Severino in the centre of the study area (2.38 MJ m^{-3} K^{-1}) passing through the municipality of Pollenza which show an average value almost intermediate between the two (2.26 MJ m^{-3} K^{-1}). The easternmost areas have the lowest SVC values due to deeper saturation levels and a more significant component of gravelly/sandy sediments, which weigh more in calculating the average SVC of the first 100 m of depth. The highest SVC values are found, instead, near Castelraimondo and Gagliole (>2.50 MJ m^{-3} K^{-1}; Fig. 5b) due to the presence of the Marnoso-Arenacea Fm, which is characterized by the highest SVC values among the substrate lithotypes occurring in the study area (Table 1). In the WSW part of the study area, the municipalities of Pioraco and Fiuminata (Fig. 5b) are characterized by intermediate values (between 2.38 and 2.50 MJ m^{-3} K^{-1}) due to the low thicknesses of the unconsolidated deposits and the presence of formations with intermediate (2.4 and 2.5 MJ m^{-3} K^{-1}) volumetric heat capacity values (i.e., Sc. Bianca-Rossa-Variegata and Marne a Fucoidi Fms; Table 1).

4.2. Specific heat extraction (SHE) and geothermal potential estimation

Using Eq. (2), it was possible to associate each lithotype in the study area with a SHE value (Table 1). The SHE map directly correlates to the λ

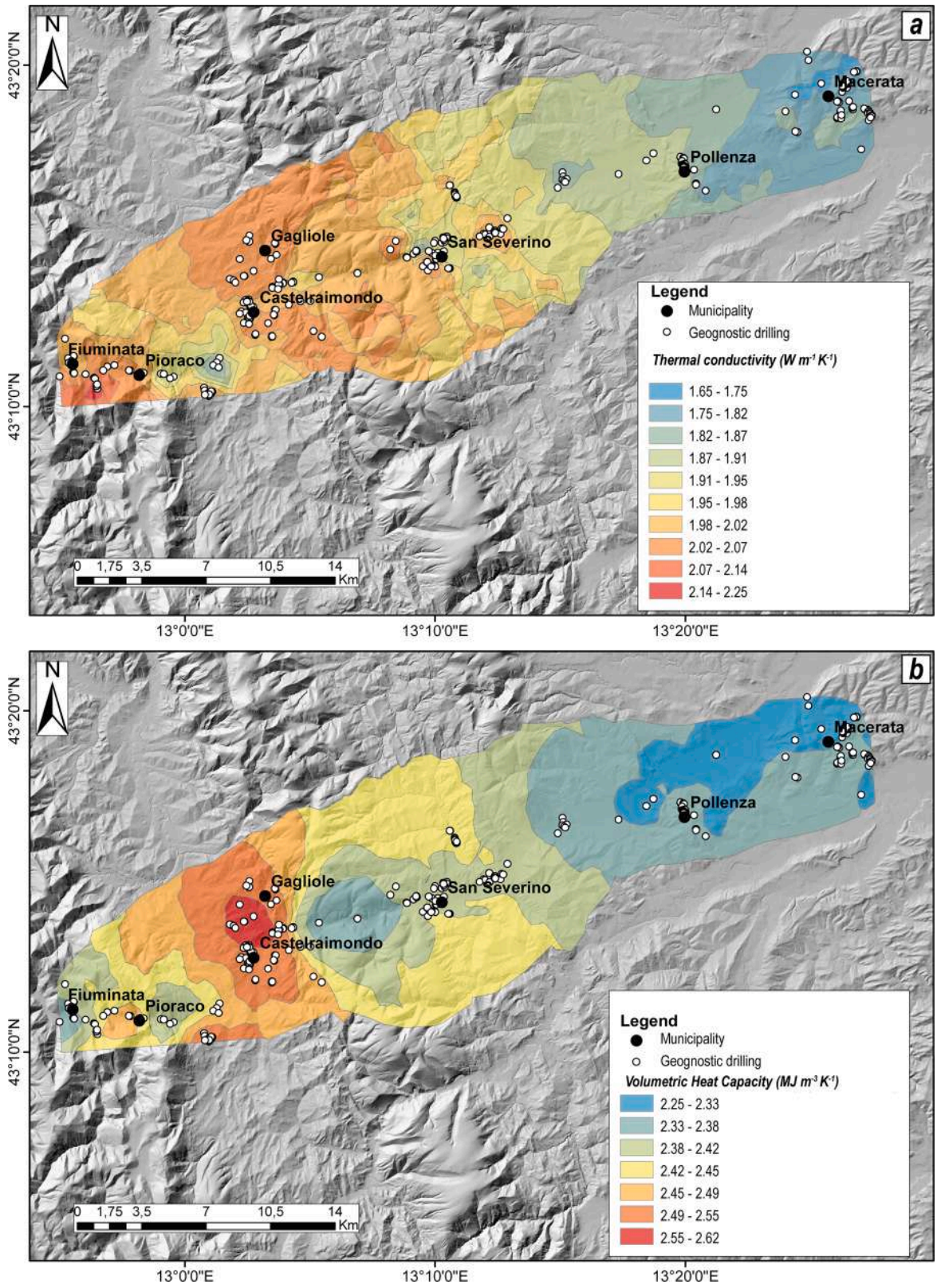

Fig. 5. Maps of the estimated a) thermal conductivity and b) volumetric heat capacity of the ground. Both are averaged over 100 m of depth from the surface.

spatial distribution because of the close relationship between the two physical properties. The minimum and maximum values calculated on the stratigraphic verticals of 100 m of depth are 3.83 and 4.86 kW. Macerata municipality shows the lowest SHE values, generally lower than 4.1 kW (Fig. 6a), due to the large presence of the Argille Azzurre Fm (42 W m^{-1}; Table 1). Moving from Macerata towards WSW, the values gradually increase to reach values >4.58 kW in the Gagliole and Castelraimondo area (Fig. 6a). The highest values (4.35–4.86 kW) were calculated at the Fiuminata municipality (Fig. 6a) derived by the presence of the marly-limestone lithologies associated with the Marne a

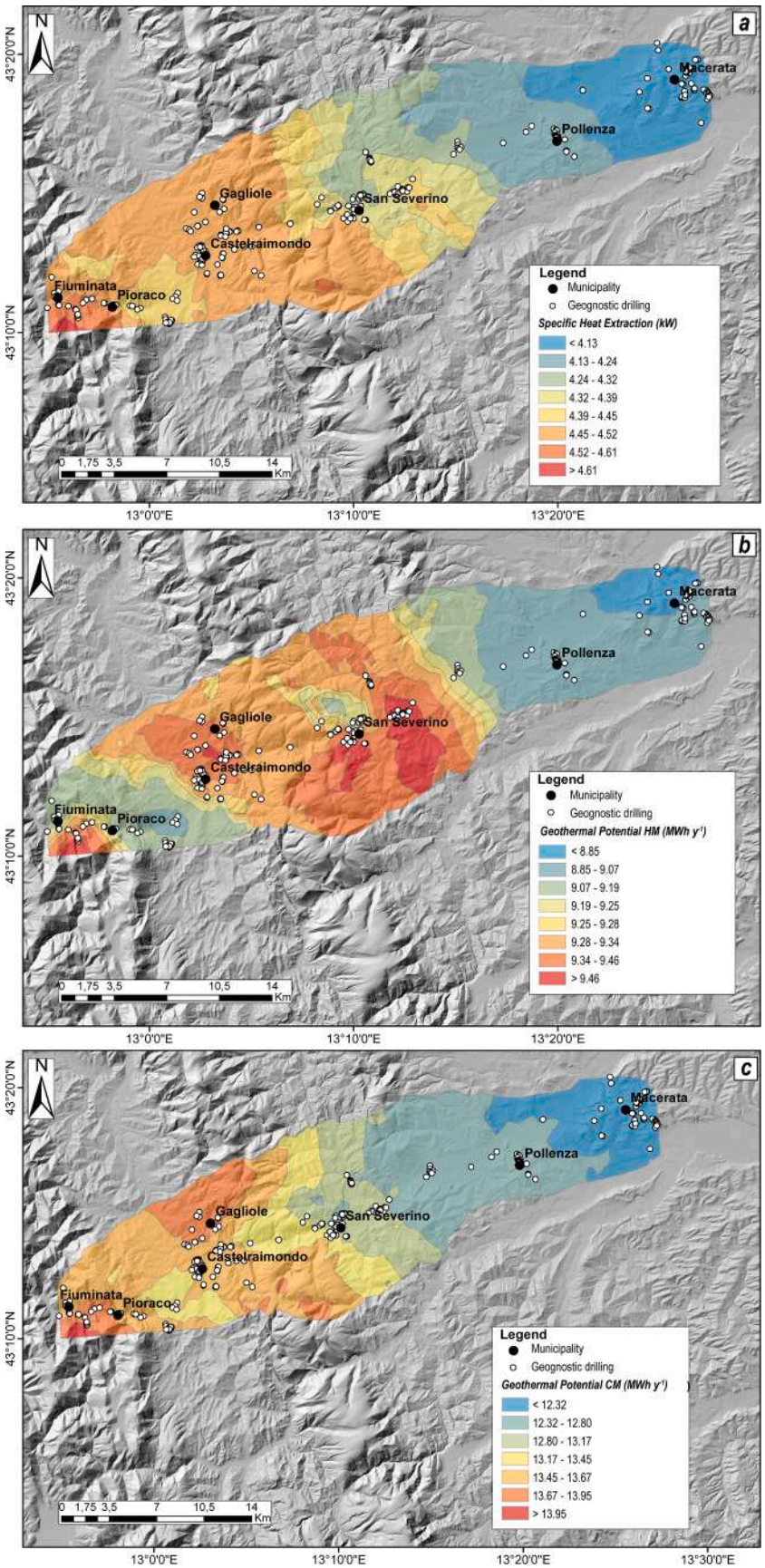

Fig. 6. Maps of the a) Specific Heat Extraction estimated for 100 m of depth BHEs, and b, c) estimated shallow geothermal potential of the study area by means of the G.POT algorithm for heating (HM) and cooling (CM) modes of operation of the closed-loop BHEs systems, respectively.

Fucoidi Fm (49 W m^{-1}; Table 1).

The shallow geothermal potential maps for heating (Fig. 6b) and cooling (Fig. 6c) were obtained using the G.POT algorithm (Casasso and Sethi, 2016). Four zones with high potential in both heating and cooling modes, corresponding to Gagliole, Castelraimondo, San Severino, and Fiuminata areas, were defined from the maps. In these zones, the values are generally >9.20 MWh y^{-1} (with a maximum of 10.12 MWh y^{-1}) and >13.00 MWh y^{-1} (with a maximum of 14.80 MWh y^{-1}) in heating and cooling modes, respectively. These values are recorded in those areas where the high thermal conductive lithologies of the Marne a Fucoidi, Scaglia Bianca-Rossa-Variegata, and Marnoso-Arenacea Fms (Table 1) outcrop or approach the surface (Fig. 1b). Despite the generally higher undisturbed temperature of the ground (Fig. 2), the lowest values (i.e., mean values <9 MW y^{-1} and <12.20 MWh y^{-1} in heating and cooling modes, respectively) are recorded in the Macerata and Pollenza areas. In fact, the higher thickness of the alluvial unconsolidated deposit in these sectors and the presence of the Argille Azzurre and Colombacci Fms, with their relatively low thermal conductivity values (Table 1), decrease the geothermal potential. The shallow geothermal potential of the Pioraco area is slight above 8.91 and 13.27 MWh y^{-1} in heating and cooling modes, respectively, and is influenced by geological formations with relatively low thermal conductivity properties (i.e., the Bisciaro Fm: 1.32 W m^{-1} K^{-1}; Table 1) although associated with the lower thickness of unsaturated sedimentary material compared to the easternmost area (Table S1). The values in the central sector of the study area are mostly comprised between 9.30 and 9.70 MWh y^{-1} and 13.20 and 13.70 MWh y^{-1} in heating and cooling modes, respectively, due to a relatively homogenous undisturbed soil temperature (11.4–13.6 °C)

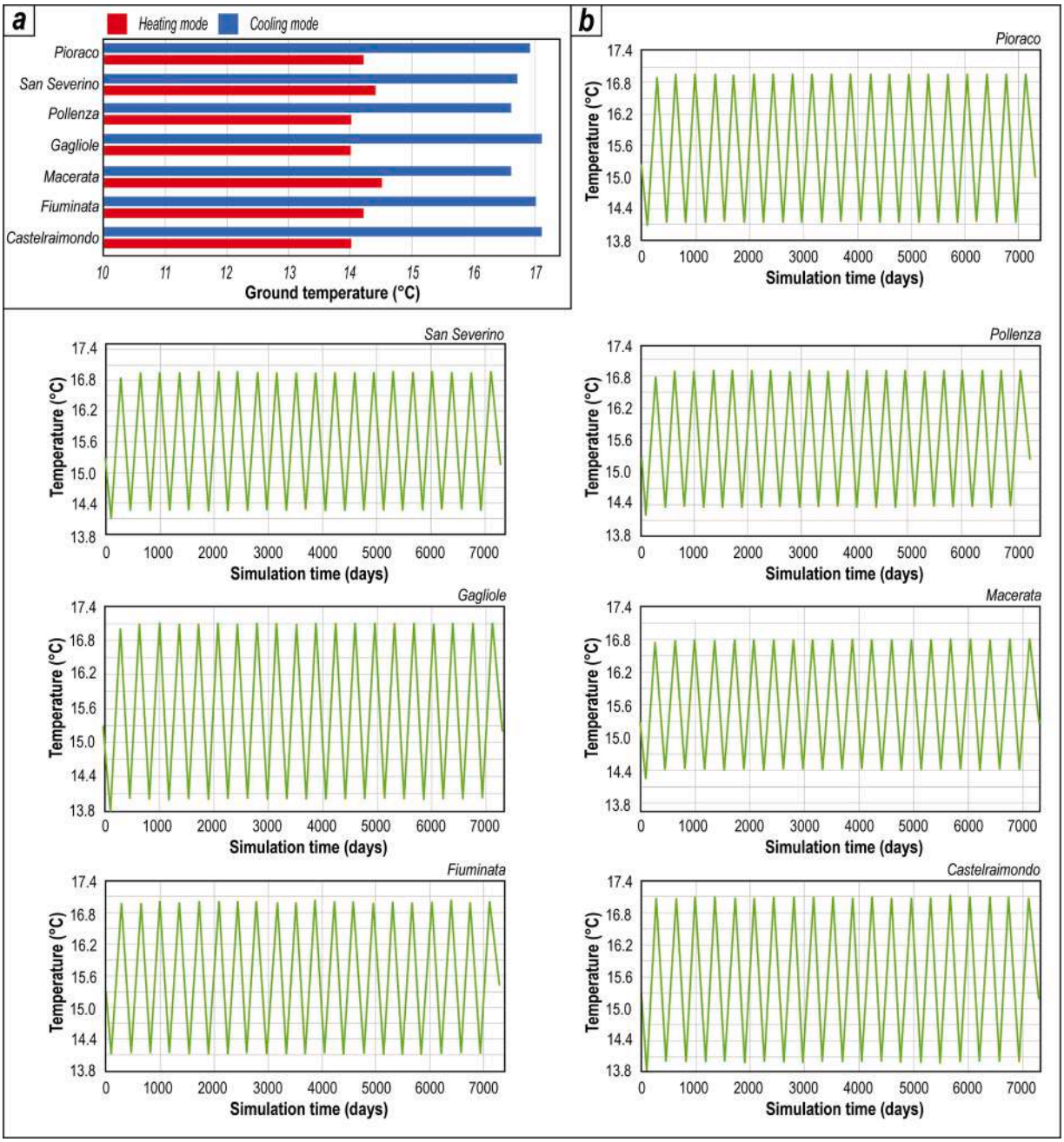

Fig. 7. a) Ground average temperature variations produced by the operation of the closed-loop BHEs systems during heating and cooling modes in the 20 years' time span interval; b) detailed seasonal variations of the ground average temperature in each simulated closed-loop BHEs system of the seven municipalities of the Potenza River valley.

(Fig. 2) and high average thermal conductivity values of the outcropping geological formations. Some differences can be highlighted when Fig. 6a, b and c are compared. These are mainly found in the San Severino and Castelraimondo areas, where high values of the G.POT are found (Fig. 6b,c) despite SHE values not being exceptionally high (Fig. 6a). Other apparent inconsistencies are found near Pioraco, where medium-high SHE values are reached, but a relatively low shallow geothermal potential for heating mode is estimated. In both cases, an important role is played by the undisturbed ground temperature that, with similar geological and thermal conditions, significantly influences the sustainability of the BHE systems and the geothermal potential.

Finally, the computed geo-exchange potential of the study area can be considered as a promising medium-high one when compared to other Italian areas where the G.POT method has been applied for heating (e.g., Casasso et al., 2017, 2018; Casasso and Sethi, 2017; Taussi et al., 2021; Vespasiano et al., 2023) and cooling (Vespasiano et al., 2023) purposes, as well as other Mediterranean areas (e.g., Ramos-Escudero et al., 2021).

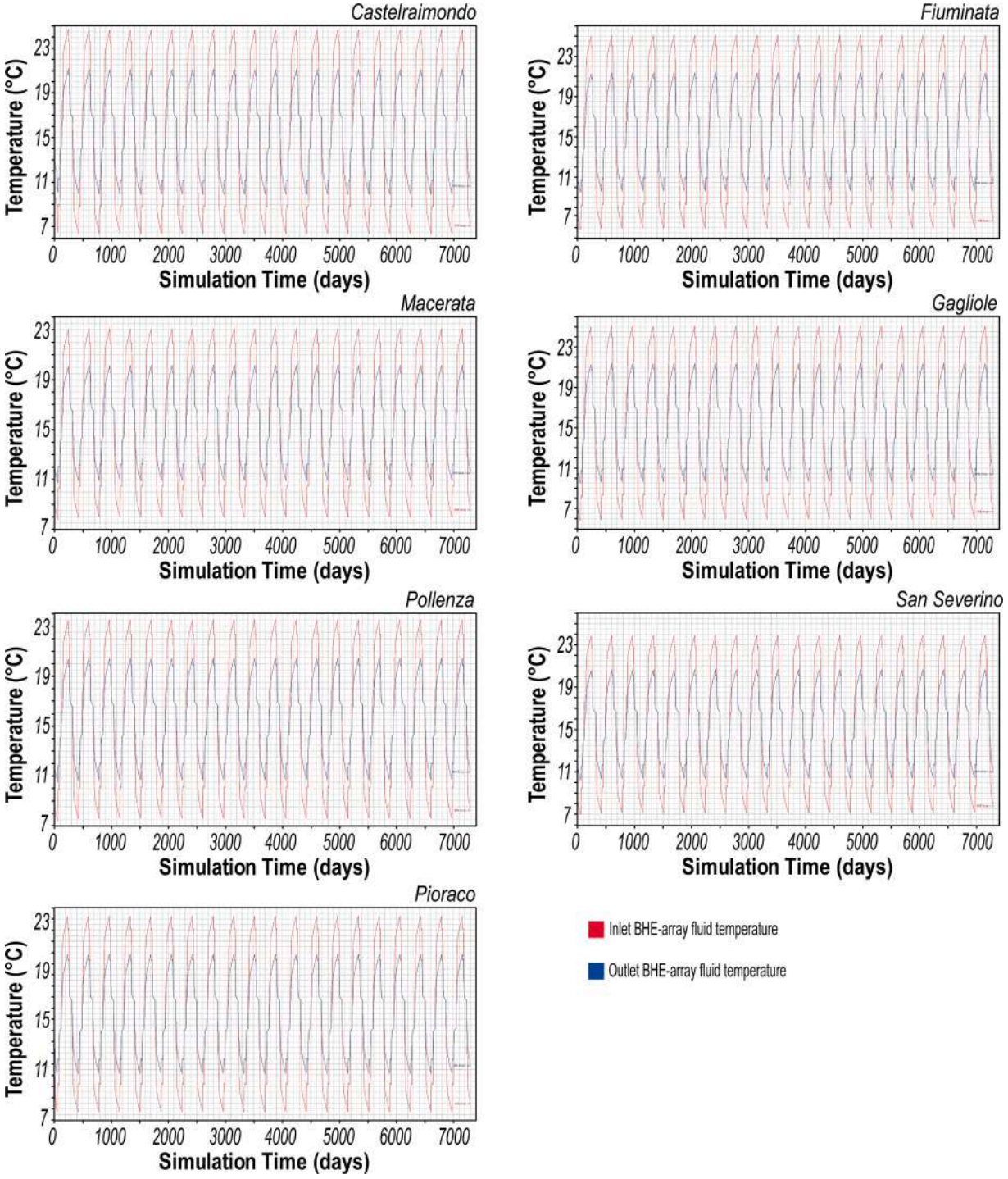

Fig. 8. Detailed diagrams of inlet (red line) and outlet (blue line) temperatures of the heat carrier fluid inside the closed-loop BHEs systems for each of the seven municipalities of the Potenza River valley.

4.3. Numerical models

The diagrams of average temperatures reported in Fig. 7 indicate the thermal plume produced by the closed-loop vertical BHEs heating and cooling system operation. The temperature was averaged between the three BHEs, with an imposed static piezometric setting and no groundwater flow. Apart from the seasonal variations due to winter-summer heat exchange inversions (Fig. 7a), the subsurface seems to reach, in the 20 years' time interval, a thermal equilibrium in all the simulated points (Fig. 7b), with minimal deviations from the undisturbed temperature only in the first few years of heating and cooling operations.

Considering the thermal plume, the low permeability of the lithotypes allows heat to be exchanged almost exclusively by conduction, producing a limited plume mainly confined to the BHEs' surroundings. The maximum ground temperatures reached in cooling mode are not very high, varying from 17.1 °C (Castelraimondo, Fiuminata, and San Severino) to 16.5 °C (Macerata), as well as the minimum ground temperatures in heating mode do not drop below 14.4 °C (Macerata and Pollenza) and 14.0 °C (Fiuminata and Gagliole). This shows a greater heat exchange between the BHEs and the ground in the Castelraimondo, Fiuminata, and San Severino municipalities than in the Macerata and Pollenza ones. Gagliole and Pioraco show an intermediate trend, with a ground average maximum temperature of 16.9 °C and 17.0 °C in cooling mode, respectively, and 14.2 °C in heating mode. Overall, the seasonal periodicity during the years shows a correct balance of heat exchange between BHEs/ground and heating and cooling modes. Neither a marked increase nor a decrease in temperature seems to be highlighted during the 20-year time interval. Therefore, the thermal plume produced seems to be balanced in all the seven municipalities of the study area and does not lead to any long-term temperature increase - or decrease - drift of the ground.

The diagrams of BHE inlet and outlet temperatures confirm the considerations made above. The municipalities of Fiuminata and Castelraimondo have the highest inlet temperatures of the heat carrier fluid flowing in the BHEs. The inlet fluid temperatures reach 25 °C in cooling and 6 °C in heating modes, respectively. Slightly different temperatures are recorded in Gagliole (24.8 °C–6.4 °C), while for the municipalities of Pioraco and San Severino, the temperatures reached are up to 24.3 °C and 24.0 °C in cooling and down to 6.8 °C and 7.0 °C in heating mode, respectively. The two municipalities that show a slightly lower attitude to heat exchange with a closed-loop BHEs system are Pollenza and Macerata, displaying 23.5 °C and 23.0 °C in cooling and 7.5 °C and 8.0 °C in heating modes, respectively. Thus, those areas showing higher differences of temperature extracted from the ground suggest more favourable conditions for BHE closed-loop systems performances regarding energy efficiency and reduction of the electrical energy to be used since the heat pump will need less power absorbed to reach the air conditioning temperatures.

The numerical model results agree with the estimated shallow geothermal potential (Fig. 6b,c). The areas with the highest geo-exchange potential (Gagliole, Castelraimondo, and Fiuminata) are also the most suitable and functional for installing a closed-loop vertical BHE plant. In these areas, the numerical models suggest a limited ground temperature variation (Fig. 7), reaching about 17.1 °C and 14.0 °C in cooling and heating mode, respectively, as well as a narrow range of temperature variations of the thermovector fluid (Fig. 8) between the incoming and outgoing fluid (3.5–3.8 and 3.7–4.2 °C in cooling and heating mode, respectively). The areas showing the lowest geothermal potential are Macerata and Pollenza for both air-conditioning modes (Fig. 6b,c). The numerical models thus match the prediction of the G.POT maps. Indeed, the average ground temperature graphs (Fig. 7) show that the reached temperatures are 16.5 and 14.4 °C in cooling and heating mode, respectively, thus suggesting a negligible long-term variation (drift). Even the measured temperature of the heat carrier fluid (Fig. 8) within the vertical BHEs shows how the ΔT of the inlet and outlet temperature is limited to 2.8 °C in both modes. The numerical simulations of the areas with intermediate shallow geothermal potential (Pioraco and San Severino; Fig. 6b,c) also show an intermediate trend. The average temperature (Fig. 7) shows that the virtual closed-loop BHEs systems installed in these areas would produce a ground temperature drift of up to 16.9 °C and 14.4 °C and 16.9 °C and 14.1 °C in cooling and heating mode at San Severino and Pioraco, respectively. The temperature graphs of the thermovector fluid (Fig. 8) also show intermediate values suggesting a ΔT of the inlet and outlet temperature of 3.7 °C at San Severino and 3.3 °C at Pioraco in heating mode, and 3.2 °C at San Severino and 3.5 °C at Pioraco in cooling mode.

5. Concluding remarks

The present research shows how publicly available geological-hydrogeological data of the ground, coupled with the thermophysical properties of the rocks, represent handy tools to estimate the shallow geothermal (geo-exchange) potential aimed at indoor air conditioning as a renewable. The geological formations of the Umbria-Marche succession occurring along the Potenza River valley show variable values of thermal conductivity driving the medium-high geothermal potential obtained with the G.POT algorithm, with values up to 10.1 MWh y^{-1} and 14.8 MWh y^{-1} for the heating and cooling mode operations respectively. Numerical models were also developed based on the average characteristics of the ground to test the sustainability of the geo-exchange throughout the seven municipalities of the study area. Three-dimensional numerical finite element models (FEFLOW software) were used to constrain the temperature dynamics of the ground and the energy efficiency of the heating and cooling systems, operated by a standard array of three closed-loop BHEs of 100 m of depth, coupled with a 12-kW heat pump. The prediction of the ground average temperatures during a long-term (20 years) operation of the standard BHEs virtual plants in a balanced mode of operation, i.e., indoor seasonal heating and cooling cycles, highlighted negligible drift compared to the pristine undisturbed ground temperature. The numerical models also closely match the results of the thematic maps of the geo-exchange potential obtained by the G.POT algorithm. This result is of paramount importance in terms of correct, renewable-based, and sustainable territorial planning in those areas interested in building restoration and reconstruction, as in the case of the post-2016 earthquake of Central Italy that hit the study area and the whole southern Marche Region. Besides not impacting the air with greenhouse gas emissions, the closed-loop BHE systems can be also considered a renewable with a long-term sustainability of the ground heat exchange. Finally, null visual impacts of the closed-loop BHE system coupled with geothermal heat pumps should develop awareness among society, designers, technicians, and policy-makers to consider the geo-exchange a first-order choice in indoor air conditioning.

CRediT authorship contribution statement

Mario Di Pierdomenico: Conceptualization, Data curation, Formal analysis, Investigation, Methodology, Visualization, Writing – original draft. **Marco Taussi:** Conceptualization, Investigation, Methodology, Project administration, Supervision, Validation, Visualization, Writing – original draft, Writing – review & editing. **Antonio Galgaro:** Methodology, Resources, Validation, Writing – review & editing. **Giorgia Dalla Santa:** Methodology, Resources, Validation, Writing – review & editing. **Massimiliano Maggini:** Data curation, Formal analysis, Methodology. **Alberto Renzulli:** Conceptualization, Funding acquisition, Methodology, Project administration, Supervision, Validation, Writing – review & editing.

Declaration of competing interest

The authors declare that they have no known competing financial interests or personal relationships that could have appeared to influence

the work reported in this paper.

Data availability

Data are reported in the supplementary material.

Acknowledgements

This work was carried out thanks to scholarships to M. Di Pierdomenico and M. Maggini financially supported by Marche Region "POR Marche FSE 2014/2020. - Asse 1- P.I. 8.1- R.A. 8.5''. A temporary licence of FEFLOW was generously granted by DHI for scientific purposes, through the University of Padova. Two anonymous reviewers are kindly thanked for their valuable comments that helped improving an early version of the manuscript. Editor-in-Chief C. Bromley is also thanked for the editorial handling.

Supplementary materials

Supplementary material associated with this article can be found, in the online version, at doi:10.1016/j.geothermics.2024.102954.

References

Alcaraz, M., Vives, L, 2023. Shallow geothermal energy resources and thermal impacts in Buenos Aires City, Argentina. In: Espinoza-Andaluz, M., Melo Vargas, E., Santana Villamar, J., Encalada-Dávila, Á (Eds.), Congress on Research, Development, and Innovation in Renewable Energies. Green Energy and Technology. Springer, Cham. https://doi.org/10.1007/978-3-031-26813-7_7.

Andújar Márquez, J.M., Martínez Bohórquez, M.A., Gómez Melgar, S., 2016. Ground thermal diffusivity calculation by direct soil temperature measurement. Application to very low enthalpy geothermal energy systems. Sensors 16, 306. https://doi.org/10.3390/s16030306.

ASTM, 1985. Standard test method for classification of soils for engineering purposes. Annual Book of ASTM Standards—Unified Soil Classification System. In: ASTM Designation D 2487-83, 04-08, 4. American Society for Testing and Materials, West Conshohocken, PA, USA, pp. 395–408.

Bayer, P., Rivera, J.A., Schweizer, D., Scharli, U., Blum, P., Rybach, L., 2016. Extracting past atmospheric warming and urban heating effects from borehole temperature profiles. Geothermics 64, 289–299.

Bayer, P., Attard, G., Blum, P., Menberg, K., 2019. The geothermal potential of cities. Renew. Sustain. Energy Rev. 106, 17–30.

Barbieri, S., Antelmi, M., Panday, S., Baratto, M., Angelotti, A., Alberti, L., 2022. Innovative numerical procedure for simulating borehole heat exchangers operation and interpreting thermal response test through MODFLOW-USG code. J. Hydrol. 614 (part B), 128556 https://doi.org/10.1016/j.jhydrol.2022.128556.

Bee, E., Prada, A., Baggio, P., Psimopoulos, E., 2019. Air-source heat pump and photovoltaic systems for residential heating and cooling: potential of self-consumption in different European climates. Build. Simul. 12, 453–463. https://doi.org/10.1007/s12273-018-0501-5.

Bigi, S., Calamita, F., Cello, G., Centamore, E., Deiana, G., Paltrinieri, W., Ridolfi, M., 1999. Tectonics and sedimentation within the Messinian foredeep in the Central Apennines, Italy. J. Pet. Geol. 22 (1), 5–18.

Blasi, A., Menichetti, M., 2012. Conducibilità termica distribuita da un test di risposta termica (TRT) su una sonda geotermica. Acque Sotter. Ital. J. Groundw. 3, 33–41.

Blasi, A, 2012. Aspetti geologici del geoscambio: test termici, profili di temperatura e monitoraggio nella geotermia a bassa entalpia. PhD thesis. University of Urbino, Italy, p. 171 in italian.

Calamita, F., Cello, G., Deiana, G., Paltrinieri, W., 1994. Structural styles, chronology rates of deformation, and time-space relationships in the Umbria-Marche thrust system (central Apennines, Italy). Tectonics 13 (4), 873–881. https://doi.org/10.1029/94TC00276.

Casasso, A., Sethi, R., 2016. G.POT: a quantitative method for the assessment and mapping of the shallow geothermal potential. Energy 106, 765–773. https://doi.org/10.1016/j.energy.2016.03.091.

Casasso, A., Sethi, R., 2017. Assessment and mapping of the shallow geothermal potential in the province of Cuneo (Piedmont, NW Italy). Renew. Energy 102, 306–315.

Casasso, A., Pestotnik, S., Rajver, D., Jež, J., Prestor, J., Sethi, R., 2017. Assessment and mapping of the closed-loop shallow geothermal potential in Cerkno (Slovenia). Energy Procedia 125, 335–344.

Casasso, A., Della Valentina, S., Di Feo, A.F., Capodaglio, P., Cavorsin, R., Guglielminotti, R., Sethi, R, 2018. Ground source heat pumps in Aosta Valley (NW Italy): assessment of existing systems and planning tools for future installations. Rend. Online Soc. Geol. Ital. 46, 59–66.

Cello G., Deiana G., Gazzadini D., Marchegiani L., Mazzoli S. (1996). Riconoscimento ed analisi di alcune associazioni di strutture sinsedimentarie pre-orogeniche in Appennino centrale. In: G. Cello, G. Deiana & P. Pierantoni (Editori), "Geodinamica e Tettonica Attiva del Sistema Tirreno-Appennino", Studi Geologici Camerti, Spec. 1995 (1): 291–303.

Chicco, J., Pierantoni, P.P., Costa, M., Invernizzi, C., 2019a. Plio-quaternary tectonics and possible implications for geothermal fluids in the Marche Region (Italy). Tectonophysics 755, 21–34.

Chicco, J., Verdoya, M., Giuli, G., Invernizzi, C., 2019b. Thermophysical properties and mineralogical composition of the Umbria-Marche carbonate succession (central Italy). In: Koeberl, C., Bice, D.M. (Eds.), 250 Million Years of Earth History in Central Italy, Celebrating 25 Years of the Geological Observatory of Coldigioco, 542. Geological Society of America, Boulder, CO, USA, pp. 59–67. https://doi.org/10.1130/2019.2542(02).

Clauser, C., 2011. Thermal storage and transport properties of rocks, II: thermal conductivity and diffusivity. In: Gupta, H.K. (Ed.), Encyclopedia of Solid Earth Geophysics. Encyclopedia of Earth Sciences Series. Springer, Dordrecht. https://doi.org/10.1007/978-90-481-8702-7_67.

Conti, P., Cornamusini, G., Carmignani, L., 2020. An outline of the geology of the Northern Apennines (Italy), with geological map at 1:250,000 scale. Ital. J. Geosci. 139, 149–194. https://doi.org/10.3301/IJG.2019.25.

Dalla Santa, G., Galgaro, A., Sassi, R., Cultrera, M., Scotton, P., Mueller, J., Bertermann, D., Mendrinos, D., Pasquali, R., Perego, R., Pera, S., Di Sipio, E., Cassiani, G., De Carli, M., Bernardi, A, 2020. An updated ground thermal properties database for GSHP applications. Geothermics 85, 101758. https://doi.org/10.1016/j.geothermics.2019.101758.

Dalla Santa, G., Pasquier, P., Schenato, L., Galgaro, A, 2022. Repeated ETRTs in a complex stratified geological setting: high-resolution thermal conductivity identification by multiple linear regression. J. Geotech. Geoenviron. Eng. 148 (4), 04022007.

Daysh, S., Carey, B., Doorman, P., Luketina, K., White, B., Zarrouk, S.J., 2021. 2015–2020 New Zealand country update. In: Proceedings World Geothermal Congress 2020+1; Reykjavik, Iceland, April - October 2021.

Della Vedova, B., Bellani, S., Pellis, G., Squarci, P, 2001. Deep temperatures and surface heat flow distribution. In: Vai, G.B., Martini, P. (Eds.), Anatomy of an Orogen: The Apennines and Adjacent Mediterranean Basins. Springer, Dordrecht, The Netherlands, pp. 65–76.

Di Sipio, E., Chiesa, S., Destro, E., Galgaro, A., Giaretta, A., Gola, G., Manzella, A., 2013. Rock thermal conductivity as key parameter for geothermal numerical models. Energy Procedia 40, 87–94. https://doi.org/10.1016/j.egypro.2013.08.011.

Diersch, H.J.G., 2014. FEFLOW, Finite Element Modeling of Flow, Mass and Heat Transport in Porous and Fractured Media. Springer, Berlin Heidelberg, Germany.

Diersch, H.J.G., Bauer, D., Heidemann, W., Ruhaak, W., Schatzl, P., 2010. Finite Element Formulation for Borehole Heat Exchangers in Modeling Geothermal Heating Systems by FEFLOW. FEFLOW White Papers vol. V. DHI-WASY, Berlin, Germany.

DPC - Dipartimento della Protezione Civile (2019). Studi di Microzonazione Sismica in Italia. Available online: https://www.comune.macerata.it/ambiente-e-territorio/protezione-civile/microzonazione-sismica/.

Eskilson, P., Claesson, J., 1988. Simulation model for thermally interacting heat extraction boreholes. Numer. Heat Transf. 13, 149–165.

Galgaro, A., Dalla Santa, G., Zarrella, A, 2021. First Italian TRT database and significance of the geological setting evaluation in borehole heat exchanger sizing. Geothermics 94, 102098.

Garcia-Gil, A., Vázquez-Suñe, E., Alcaraz, M.M., Serrano Juan, A., Sánchez-Navarro, J.Á., Montlleó, M., Rodríguez, G., Lao, J., 2015. GIS-supported mapping of low-temperature geothermal potential taking groundwater flow into account. Renew. Energy 77, 268–278.

Gemelli, A., Mancini, A., Longhi, S., 2011. GIS-based energy-economic model of low temperature geothermal resources: a case study in the Italian Marche region. Renew. Energy 36, 2474–2483. https://doi.org/10.1016/j.renene.2011.02.014.

Gigot, V., Francois, B., Huysmans, M., Gerard, P., 2023. Monitoring of the thermal plume around a thermally activated borehole heat exchanger and characterization of the ground hydro-geothermal parameters. Renew. Energy 218, 119250. https://doi.org/10.1016/j.renene.2023.119250.

Gizzi, M., Taddia, G., Cerino Abdin, E., Lo Russo, S., 2020. Thermally affected zone (TAZ) assessment in open-loop low-enthalpy groundwater heat pump systems (GWHPs): potential of analytical solutions. Geofluids 2020, 2640917. https://doi.org/10.1155/2020/2640917.

Hałaj, E., Pająk, L., Papiernik, B., 2020. Finite element modeling of geothermal source of heat pump in long-term operation. Energies 13, 1341. https://doi.org/10.3390/en13061341.

Hecht-Méndez, J., de Paly, M., Beck, M., Bayer, P., 2013. Optimization of energy extraction for vertical closed-loop geothermal systems considering groundwater flow. Energy Convers. Manag. 66, 1–10. https://doi.org/10.1016/j.enconman.2012.09.019.

INGV - Istituto Nazionale di Geofisica e Vulcanologia (2016). Bollettino Sismico Italiano INGV. Available at: http://cnt.rm.ingv.it/event/8863681.

ISTAT (2021). Dati del Censimento della Popolazione e delle Abitazioni 2018 (Italian Population Census). Available online: http://dati-censimentipermanenti.istat.it/#.

Kerme, E.D., Fung, A.S., 2021. Heat transfer analysis of single and double U-tube borehole heat exchanger with two independent circuits. J. Energy Storage 43, 103141. https://doi.org/10.1016/j.est.2021.103141.

Liso, V., Zhao, Y., Brandon, N., Pagh Nielsen, M., Knudsen Kær, S., 2011. Analysis of the impact of heat-to-power ratio for a SOFC-based mCHP system for residential application under different climate regions in Europe. Int. J. Hydrogen Energy 36 (21), 13715–13726. https://doi.org/10.1016/j.ijhydene.2011.07.086.

Lund, J.W., Toth, A.N., 2021. Direct utilization of geothermal energy 2020 worldwide review. Geothermics 90, 101915.

Manzella, A., Bonciani, R., Allansdottir, A., Botteghi, S., Donato, A., Giamberini, S., Lenzi, A., Paci, M., Pellizzone, A., Scrocca, D., 2018. Environmental and social aspects of geothermal energy in Italy. Geothermics 72, 232–248. https://doi.org/10.1016/j.geothermics.2017.11.015.

Marcheggiani, L., Bertotti, G., Cello, G., Deiana, G., Mazzoli, S., Tondi, E., 1999. Pre-orogenic tectonics in the Umbria-Marche sector of the Afro-Adriatic continental margin. Tectonophysics 315, 123–143.

Menichetti, M., Renzulli, A., 2009. Geotermia a bassa entalpia e misure di temperature in pozzo—Low enthalpy geothermal resources and temperature measurements. Rend. Online Soc. Geol. Ital. 6, 333–334.

Menichetti, M., Renzulli, A., Piscaglia, F., Blasi, A., 2009. Geotermia a bassa entalpia: temperatura e conducibilità termica del sottosuolo. In: Sistemi Avanzati di Produzione per Geotermia. Energy Resources, Ancona. pp. 80–39.

Morris, D.A., Johnson, A.I., 1967. Report, Water Supply Paper 1839-D. The U.S. Government Printing Office, p. 42. https://doi.org/10.3133/wsp1839D published by.

Moscatelli, M., Albarello, D., Scarascia Mugnozza, G., Dolce, M., 2020. The Italian approach to seismic microzonation. Bull. Earthq. Eng. 18, 5425–5440.

Muñoz, M., Garat, P., Flores-Aqueveque, V., Vargas, G., Rebolledo, S., Sepúlveda, S., Daniele, L., Morata, D., Parada, M.A., 2015. Estimating low-enthalpy geothermal energy potential for district heating in Santiago basin-Chile (33.5°S). Renew. Energy 76, 186–195. https://doi.org/10.1016/j.renene.2014.11.019.

Muñoz, M., Aravena, D., García, K., Hurtado, N., Micco, E., Morata, D., 2023. Groundwater Heat Pump assessment operation in three cities of south–central Chile: an approach based on aquifer characterization and analytical calculations of thermal affectation zone. J. South Am. Earth Sci. 121, 104135.

Nanni, T., 1985. Le Falde di Subalveo Delle Marche: Inquadramento Idrogeologico, Qualità Delle Acque Ed Elementi di Neotettonica, 104. Ed. Regione Marche, Materiali e Programmazione, Ancona, p. ff. 22.

Pauselli, C., Gola, G., Mancinelli, P., Trumpy, E., Saccone, M., Manzella, A., Ranalli, G., 2019. A new surface heat flow map of the Northern Apennines between latitudes 42.5 and 44.5 N. Geothermics 81, 39–52. https://doi.org/10.1016/j.geothermics.2019.04.002.

Perego, R., Dalla Santa, G., Galgaro, A., Pera, S, 2022. Intensive thermal exploitation from closed and open shallow geothermal systems at urban scale: unmanaged conflicts and potential synergies. Geothermics 103, 102417. https://doi.org/10.1016/j.geothermics.2022.102417.

Piscaglia, F., Blasi, A., Del Moro, S., Polonara, F., Arteconi, A., Zanarelli, L., Renzulli, A., 2016. Monitoring of a vertical borehole ground-coupled heat pump system: a case study from a marly-limestone heat reservoir (Urbino, Central Italy). Geothermics 62, 61–69.

PTA - Piano Tutela Acque Regione Marche (2002). Available online: https://www.regione.marche.it/RegioneUtile/Ambiente/Tuteladelle-acque/PTA.

Ramos-Escudero, A., García-Cascales, M.S., Urchueguía, J.F., 2021. Evaluation of the shallow geothermal potential for heating and cooling and its integration in the socioeconomic environment: a case study in the Region of Murcia, Spain. Energies 14, 5740. https://doi.org/10.3390/en14185740.

Ricci, Lucchi F., 1986. In: Allen, P.A, Homewood, P (Eds.), The oligocene to recent Foreland Basins of the Northern Apennines. In: “Foreland Basins” book (1986). Wiley.

Rivera, J.A., Blum, P., Bayer, P., 2017. Increased ground temperatures in urban areas: estimation of the technical geothermal potential. Renew. Energy 103, 388–400.

Sáez Blázquez, C., Maté-González, M.A., Nieto, I.M., Farfán Martín, A., González-Aguilera, D, 2022. Assessment of the geothermal potential in the region of Ávila (Spain): an integrated and interactive thermal approach. Geothermics 98, 102294.

Santini, S., Basilici, M., Invernizzi, C., Jablonska, D., Mazzoli, S., Megna, A., Pierantoni, P.P., 2021. Controls of radiogenic heat and moho geometry on the thermal setting of the Marche Region (Central Italy): an analytical 3D geothermal model. Energies 14, 6511. https://doi.org/10.3390/en14206511.

Sarbu, I., Sebarchievici, C., 2014. General review of ground-source heat pump systems for heating and cooling of buildings. Energy Build 70, 441–454. https://doi.org/10.1016/j.enbuild.2013.11.068.

Schiermeier, Q., Tollefson, J., Scully, T., Witze, A., Morton, O., 2008. Energy alternatives: electricity without carbon. Nature 454 (7206), 816–823. https://doi.org/10.1038/454816a.

Soltani, M., Kashkoolia, F.M., Dehghani-Sanij, A.R., Kazemi, A.R., Bordbar, N., Farshchi, M.J., Elmi, M., Gharalif, K., Dusseault, M.B., 2019. A comprehensive study of geothermal heating and cooling systems. Sustain. Cities Soc. 44, 793–818.

Tarquini, S., Isola, I., Favalli, M., Battistini, A., 2023. TINITALY, a Digital Elevation Model of Italy with a 10 Meters Cell Size (Version 1.1). Istituto Nazionale di Geofisica e Vulcanologia (INGV). https://doi.org/10.13127/tinitaly/1.1.

Taussi, M., Borghi, W., Gliaschera, M., Renzulli, A., 2021. Defining the shallow geothermal heat-exchange potential for a lower fluvial plain of the Central Apennines: the Metauro Valley (Marche Region, Italy). Energies 14, 768. https://doi.org/10.3390/en14030768.

Tavarnelli, E., 1997. Structural evolution of a foreland fold-and-thrust belt: the Umbria-Marche Apennines, Italy. J. Struct. Geol. 19 (3–4), 523–534. https://doi.org/10.1016/S0191-8141(96)00093-4.

TCSM, 2018. Technical commission for seismic microzonation. Graphic and Data Archiving Standards. Version 4.1. National Department of Civil Protection, Rome, Italy. Available online: www.centromicrozonazionesismica.it/it/download/send/26-standardms-41/71-standardms-4-1.

USR (2016). Ufficio Speciale per la Ricostruzione – Regione Marche. Available online at: https://www.regione.marche.it/Regione-Utile/Ricostruzione-Marche/Ufficio-Speciale-per-la-Ricostruzione-Marche.

VDI 4640 (2001). German Guidelines: thermal Use of the Underground. Available online: https://www.antpedia.com/standard/6266555-8.html.

Verdoya, M., Chiozzi, P., 2018. Influence of groundwater flow on the estimation of subsurface thermal parameters. Int. J. Earth Sci. 107, 137–144.

Verdoya, M., Pacetti, C., Chiozzi, P., Invernizzi, C., 2018. Thermophysical parameters from laboratory measurements and in-situ tests in borehole heat exchangers. Appl. Eng. 144, 711–720. https://doi.org/10.1016/j.applthermaleng.2018.08.039.

Verdoya, M., Chiozzi, P., Gola, G., 2021. Unravelling the terrestrial heat flow of a young orogen: the example of the Northern Apennines. Geothermics, 101993. https://doi.org/10.1016/j.geothermics.2020.101993.

Vespasiano, G., Cianflone, G., Taussi, M., De Rosa, R., Dominici, R., Apollaro, C., 2023. Shallow geothermal potential of the Sant’Eufemia plain (South Italy) for heating and cooling systems, a potential solution in a climate-changing society. Geosciences 13 (4), 110. https://doi.org/10.3390/geosciences13040110.

Vezzani, L., Festa, A., Ghisetti, F.C., 2010. Geology and tectonic evolution of the Central–Southern Apenninnes, Italy. Geol. Soc. Am. Spec. Pap. 469, 58.

Viesi, D., Galgaro, A., Visintainer, P., Crema, L., 2018. GIS-supported evaluation and mapping of the geo-exchange potential for vertical closed-loop systems in an Alpine valley, the case study of Adige Valley (Italy). Geothermics 71, 70–87. https://doi.org/10.1016/j.geothermics.2017.08.008.